Cell Tissue Res. 201, 101–127 (1979)

Cell and Tissue Research

Activation of Human T-Lymphocytes

A Kinetic and Stereological Study

G.E. Petrzilka* and H.E. Schroeder

Department of Oral Structural Biology, Dental Institute of Zürich, Zürich, Switzerland

Summary. Stereological data of phytohaemagglutinin (PHA)-activated human T-lymphocytes were recorded at intervals (12 to 72 h) together with biochemical (isotope-uptake, lymphotoxin-release) and morphological measurements. About 98% of the cells were activated 12 h after PHA-stimulation. The activation phase lasted less than 48 h, i.e., cells entering the activation phase within 12 h were at their activation maximum by 48 h. The activated cell increased in size. The nuclear/cytoplasmic-ratio decreased. Most of the cytoplasmic organelles developed in phase with the increase of cytoplasmic volume. After 48 h, mitotic figures were frequently seen. Due to the increasing number of secondary, activated daughter cells, parameters of most cytoplasmic components declined between 48 and 72 h. Structural changes in the nucleus preceded the ^{3}H-leucine uptake, which had not reached its maximum after 72 h of incubation. The ^{3}H-leucine uptake started as early as 12 h after culture initiation, and its increase was proportional to the increasing polyribosome density. No maximum uptake was reached up to 72 h, but the development of structural components related to this uptake was at its maximum at the end of the activation phase (48 h). The formation of bound ribosomes occurred subsequent to the enlargement of the surface of the rough endoplasmic reticulum. Initial polysome formation occurred at the expense of existing free ribosomes.

Key words: T-lymphocytes – Cell activation – Stereology – Electron microscopy.

Cell activation is a process that is initiated by a stimulatory event and whereby cells undergo a series of functional changes. These changes normally include an

Send offprint requests to: Dr. H.E. Schroeder, Department of Oral Structural Biology, Dental Institute, University of Zürich, Plattenstraße 11, 8028 Zürich, Switzerland

* Dr. G.E. Petrzilka's present address is: Department of Oral Microbiology and General Immunology, Dental Institute, University of Zürich, Zürich, Switzerland

0302-766X/79/0201/0101/$05.40

enhanced physiological activity and a conspicously altered morphology. Cell division may be (but not necessarily is) a consequential feature. The stimulating or trigger event is commonly induced by any of a variety of substances, i.e., antigens, mitogens, various mediators such as lymphokines and hormones, and cell membrane components. In this broad sense, cell activation occurs in a number of different cells such as monocytes, fibroblasts, osteocytes, mast cells and lymphocytes. In connection with lymphocyte activation, both terms, stimulation and activation, often have been used synonymously (Ling and Kay, 1975). In this study, therefore, stimulation is used for the initial signal delivery, i.e., the combination of a stimulator with the receptor, while activation denotes the set of changing physiological and morphological parameters, i.e., the cellular processes responding to stimulation.

Small, non-dividing lymphocytes are particularly appropriate for studying the activation process because metabolic, functional and morphological parameters undergo large-scale changes. Another advantage of using lymphocytes is the ease of collection and separation of these cells. Although rather homogeneous lymphocyte populations can be collected, the response of such cells unfortunately lacks synchronism.

In order to perform an elaborate activation analysis, it is necessary to submit a pure and rather homogeneous cell population to a versatile methodology. A large number of investigations have utilized either morphological (Biberfeld, 1971a; Biberfeld, 1971b; Biberfeld and Johansson, 1975; Grossi et al., 1978) or quantitative biochemical methods in order to characterize the lymphocyte activation process (Cooper, 1977; Cooper and Braverman, 1977; Wedner and Parker, 1976). Only a few publications are available reporting on a partially integrated approach combining morphological and some biochemical aspects (Grossi et al., 1978; Moretta et al., 1977; Sören and Biberfeld, 1973). Most of the planimetric, karyometric, cytophotometric as well as quantitative, stereological studies have been performed using a mixed lymphocyte population (Douglas et al., 1973; Konwinski and Kozlowski, 1972; Takahashi, 1976). Although the report of Biberfeld (1971b), based on planimetric-histochemical and ultrastructural methods, has contributed much to our understanding of the cytochemical and morphological aspects of the activation process of human T-lymphocytes, extensive correlated quantitative stereological and biochemical investigations are still lacking.

The aim of this study was an attempt to provide integrated biological (i.e., metabolic and morphological) information on the activation process of phytohaemagglutinin (PHA)-stimulated T-lymphocytes, cultured over varying periods of time. Stereological data of non-activated, small T-lymphocytes have been reported recently (Petrzilka et al., 1978).

Materials and Methods

Material of Investigation

Two to four samples of 50 to 60 ml of human peripheral blood from four clinically healthy males aged 33 to 36 years were collected in a series of 10 ml glass tubes containing 10 UI/ml heparin (VITRUM, Sweden). None of the subjects was under the influence of drugs.

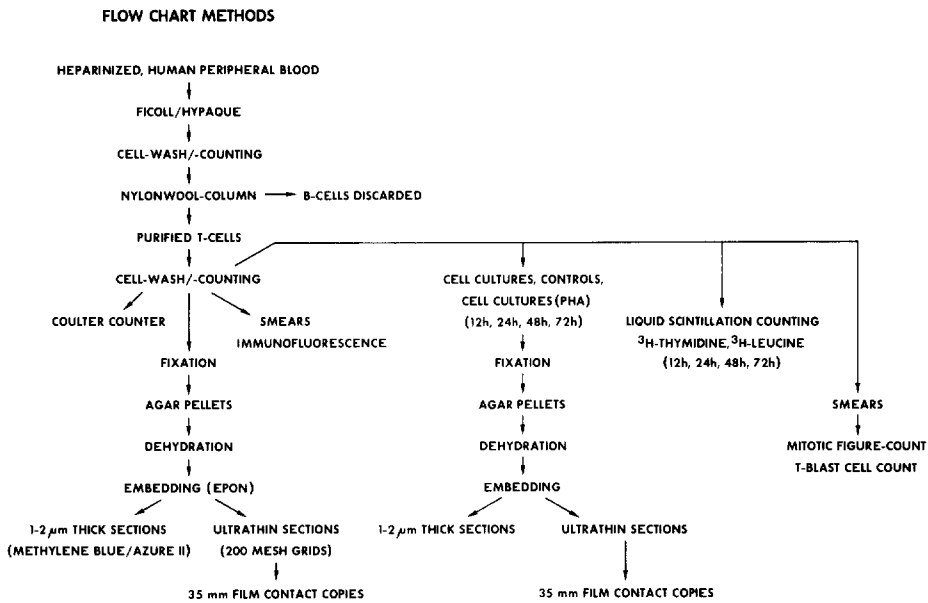

Fig. 1. Flow diagram indicating cell separation and cell processing

Mitogen

Phytohaemagglutinin-P (PHA-P; 3110-57, Lot 584 594, Difco Lab., Detroit, MI, USA) was used in an optimal concentration of 10 µg/ml. This dose was derived from a dose-response curve established in preliminary tests on T-lymphocyte suspensions with mitogen doses of 2.5, 5, 10, 15, 20 and 40 µg/ml, respectively.

Separation and Culture of T-Lymphocytes

Harvest and preparation of T-lymphocyte suspensions were described previously (Petrzilka et al., 1978). Cell preparation and processing is shown schematically in Fig. 1. Cells serving for morphometric analysis were cultured in RPMI-1640 medium supplemented with 10% autologuous plasma in Falcon tubes (Falcon 2005, Falcon Plastics, Los Angeles, CA, USA). These cells were diluted to a concentration of 1×10^6 cells/ml. Aliquots of 1 ml cell suspension each were distributed in series of six tubes. Cells of three tubes per incubation time were stimulated by adding 10 µg/ml PHA-P each. Three control cultures per incubation time were kept in aliquots of medium without PHA-P. Test and control tubes were incubated at 37° C in 5% CO_2 and 95% air. The incubation time was 12 (T_{12}), 24 (T_{24}), 48 (T_{48}) and 72 (T_{72}) h. Half of the supernatant medium was replaced after the first 24 h of incubation and subsequently every 12 h by fresh medium without PHA-P.

Radioactive Labeling

Microtest plates (Falcon 3040/41) were used for assessing the in-vitro uptake of ^{3}H-thymidine (^{3}H-dThd) and ^{3}H-leucine (^{3}H-Leu). Each "well" contained 10^5 cells in 0.1 ml medium. Test cultures received 0.1 ml PHA-P (20 µg/ml), control cultures an aliquot of medium without mitogen. All cultures were set up in 12 replicates and incubated for 12, 24, 48 and 72 h.

Four hours prior to terminating the incubation period, cells of the test and control cultures were

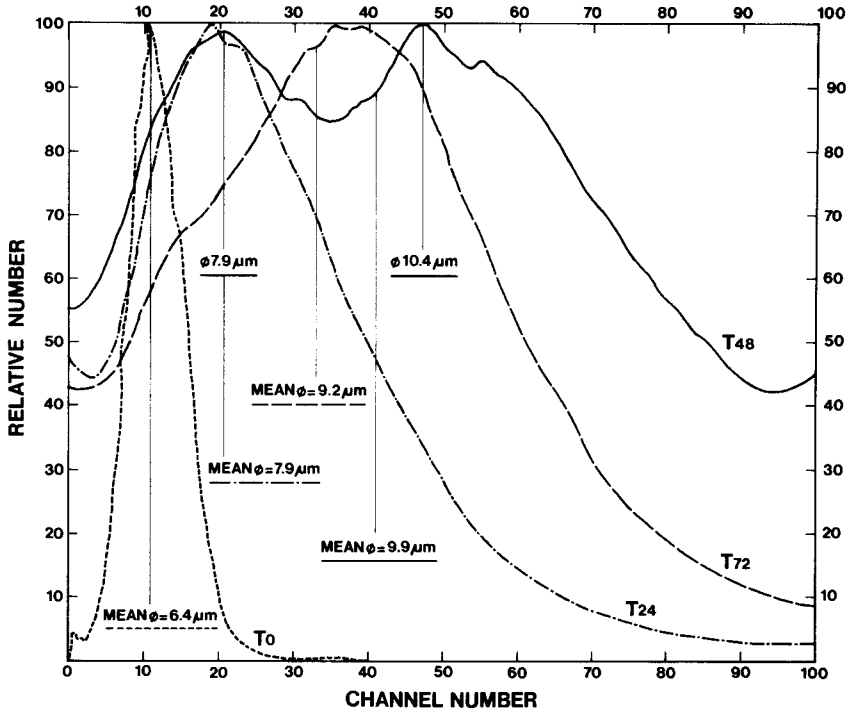

Fig. 2. Volume distribution curves and average cell diameters of small (T_0) and PHA-activated (T_{24}, T_{48}, T_{72}) T-lymphocytes. X-axis: Channel number indicates relative cell volume

pulsed with 0.2 µl ^{3}H-dThd (Methyl-^{3}H-dThd, NET-027A, 2Ci/mM, Lot 259, New England Corp. (NEN), Boston, MA, USA) or with 2 µl ^{3}H-Leu (50 Ci/mM, Lot 798 194, NEN), diluted in 50 µl medium each.

Stereological and kinetic studies were performed concomitantly, using cells of the same subject and blood sample. For technical reasons, experiments were carried out setwise, one blood sample serving for stereological and kinetic assays of two time periods only (i.e., 12 and 24, and 48 and 72 h, respectively).

Estimation of Radioactivity

Uptake of ^{3}H-dThd and ^{3}H-Leu was measured directly after the termination of each of the four culture periods. Cell processing followed the outline given by Burckhardt et al. (1977). Radioactivity was assessed with a LKB Wallac 81'000 liquid scintillation spectrometer. Results were expressed as mean and standard deviations (dpm ± s) over 12 replicates.

Cytotoxicity Assay

Lymphotoxin activity of lymphocyte-culture-supernatants from PHA-P-activated (24, 42, 48, 66 and 72 h) and non-activated T-lymphocytes was assayed at the Center for Research in Oral Biology, University of Washington, Seattle, USA. The cells of one subject were cultured in plastic tubes under the above-mentioned conditions. The medium was replaced at each time point and the supernatant collected and stored at −70° C. A modification (Spofford et al., 1974) of the ^{51}Cr-release assay of Peter and Feldman (1972) was used, employing α-L-fibroblasts as target cells (obtained from Dr. G.A. Granger,

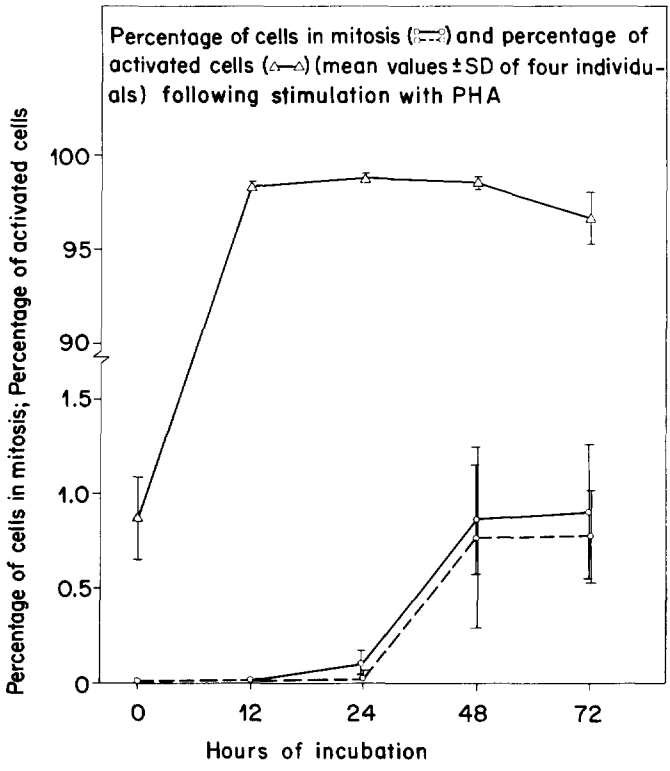

Fig. 3. Percentage of activated and dividing cells at various time points after culture initiation. The solid line (with circles) represents data derived from semithin sections; the dashed line (with circles), data from cytocentrifuge smears

Dept. Biochemistry, University California, Irvine, Ca.). A saline suspension of 10^7 fibroblasts/ml was labeled with 400 µCi $Na_2{}^{51}CrO_4$ (specific activity, 200 to 500 Ci/g of chromium, New England Nuclear Corp., Boston, Ma, USA). After washing twice in PBS, the cells were resuspended in 10 ml medium containing 5 µl/ml mytomycin C. Aliquots of 0.1 ml cell suspension containing 10^4 cells were distributed into "wells" of Falcon 3040 Micro Test II plates and incubated for 4 h. The culture medium was then replaced by 0.2 ml of the lymphocyte-test supernatant (diluted 1 : 20 with medium), supplemented by mytomycin C, and the plates were reincubated for 24 h. At the end of the incubation period the supernatants were removed and assayed for radioactivity in a gamma counter. Maximal release of radioactivity was determined by lysis of labeled cells with 10% sodium dodecyl sulphate. Percentage chromium release (PR) was calculated according to the formula of Peter and Feldman (1972). Corrected percentage release was determined by substracting the percentage release of unstimulated culture supernatant from the percentage release of experimental supernatant.

Cell-Size Determination

Cell-size of PHA-P-activated T-lymphocytes of one subject was determined prior to (T_0) and after 24, 48 and 72 h of incubation by coulter counter techniques (Coulter Electronics). The respective size distributions are presented in Fig.2.

Fixation, Embedding and Cytocentrifuge Smears

Cells were processed for light (LM) and electron microscopy (EM) as described previously (Petrzilka et al., 1978). Cytocentrifuge smears were prepared from each of the T-lymphocyte samples tested. A 0.5 ml

cell suspension containing 5×10^5 cells/ml was processed in a Shandon Eliott Centrifuge, at 1000 rpm for 10 min. The resulting smears were air-dried, fixed for 3 min in methanol and stained for 2 min in a filtered May-Grünwald solution (Merck). Following a wash in 0.02 M Sörensen phosphate buffer (pH 6.8), the smears were restained for 20 min in a double-filtered Giemsa-solution (Merck; 3 ml Giemsa: 7 ml H_2O).

Percentage of Dividing and Non-dividing, Activated Cells

A total of 48 semithin sections (1 section per block, 3 blocks per subject) and 16 cytocentrifuge smears were analyzed using the sampling microscope (Wild M-501) as described recently (Petrzilka et al., 1978). The percentage of cells in mitosis as well as that of non-dividing, but activated cells was determined (Fig. 3).

Stereological Methods

Stereological analysis was performed by utilizing a stereological model system for free spherical cells (Petrzilka et al., 1978). Random ultrathin sections (1 section per block, 3 blocks per subject and time period), on the average 54 nm thick, served for sampling electron micrographs in a hierarchical manner on three levels of magnification. In total, 1590 electron micrographs were subjected to morphometric point counting (Petrzilka et al., 1978). Non-activated T-lymphocytes and rare B-blasts present within activated cell populations were excluded from counting. All activated cells were pooled rather than further subgrouped. Calculations of the stereological parameters were performed with a Hewlett Packard 9830A calculator using the Basic-Plus program "CELLANAL" for automatic data processing (Petrzilka et al., 1978). Results were expressed in relation to absolute and relative reference compartments (i.e., the original cell volume, unit volumes of 1000 μm^3 each for the cell, the nucleus and the cytoplasm, respectively). For comparison, control data of non-activated, small T-lymphocytes (T_0) were used (Petrzilka et al., 1978).

Results

Morphology of Activated T-Lymphocytes

Shape and Size. PHA-stimulated cells were agglutinated already after 12 h of incubation. They varied considerably in shape throughout the activation period, in particular after 48 and 72 h. The number of cytoplasmic microvilli decreased. The cell diameter increased up to 48 h (Fig. 2). When calculated from stereological data, the respective diameters for the subject used in Fig. 2 were $6.3 \pm 0.3\,\mu m$ (T_0), $8.4 \pm 0.2\,\mu m$ (T_{24}), $10.2 \pm 0.6\,\mu m$ (T_{48}), and $8.6 \pm 0.2\,\mu m$ (T_{72}). Stereological averages over all four subjects were $5.8 \pm 0.4\,\mu m$ (T_0), $8.3 \pm 0.3\,\mu m$ (T_{24}), $10.0 \pm 0.2\,\mu m$ (T_{48}), $9.1 \pm 0.4\,\mu m$ (T_{72}).

In contrast, the nuclear shape did not appear to change (Figs. 4a, 5a, 7a, 8b). Nuclei were usually spherical, some being lobulated and indented. The average nuclear diameter increased from $4.5 \pm 0.3\,\mu m$ (T_0) to a maximum of $6.9 \pm 0.1\,\mu m$ (T_{48}).

Percentage of Dividing and Non-dividing, Activated Cells

T_0-cultures contained, on the average, $0.9 \pm 0.2\%$ activated cells. After 12 h of incubation, 98.4% of the cells were activated. This percentage remained constant up to 48 h and dropped slightly in T_{72}-cultures (Fig. 3).

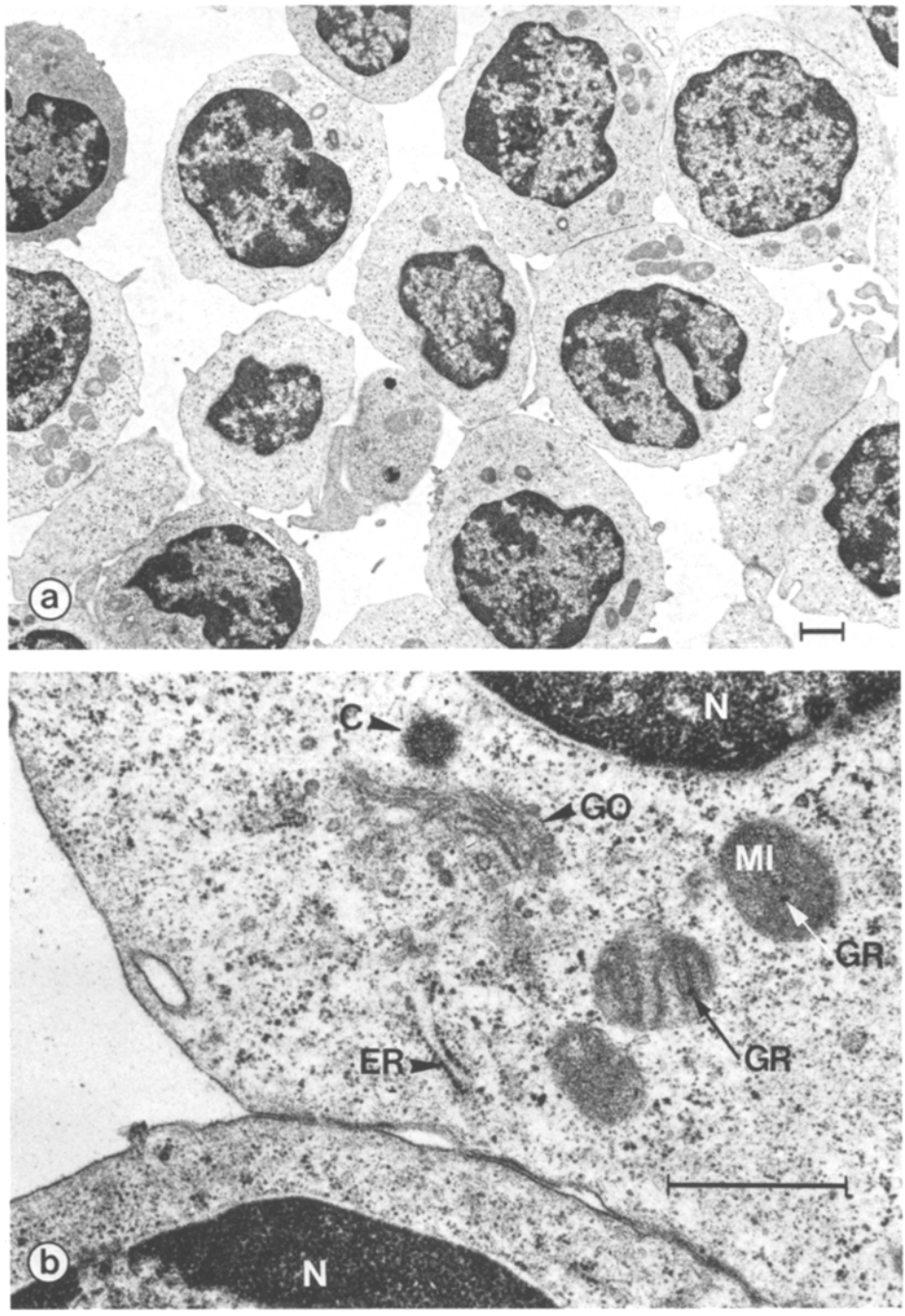

Fig. 4a and b. Ultrastructure of a T-lymphocyte aggregate 12 h after PHA-stimulation. **a** Nuclei contain eu- and heterochromatin in roughly equal amounts; nucleoli appear occasionally. The cytoplasmic seam is relatively broad. Bar, 1 μm. ×5,265. **b** Nuclear (*N*) and cytoplasmic portions with electron lucent cytoplasmic ground substance, mitochondria (*MI*) with intramitochondrial granules (*GR*), cisternae of the rough endoplasmic reticulum (*ER*) and the Golgi apparatus (*GO*), and a centriole (*C*). Single free ribosomes are more numerous than polyribosomes. Bar, 1 μm. ×23,652

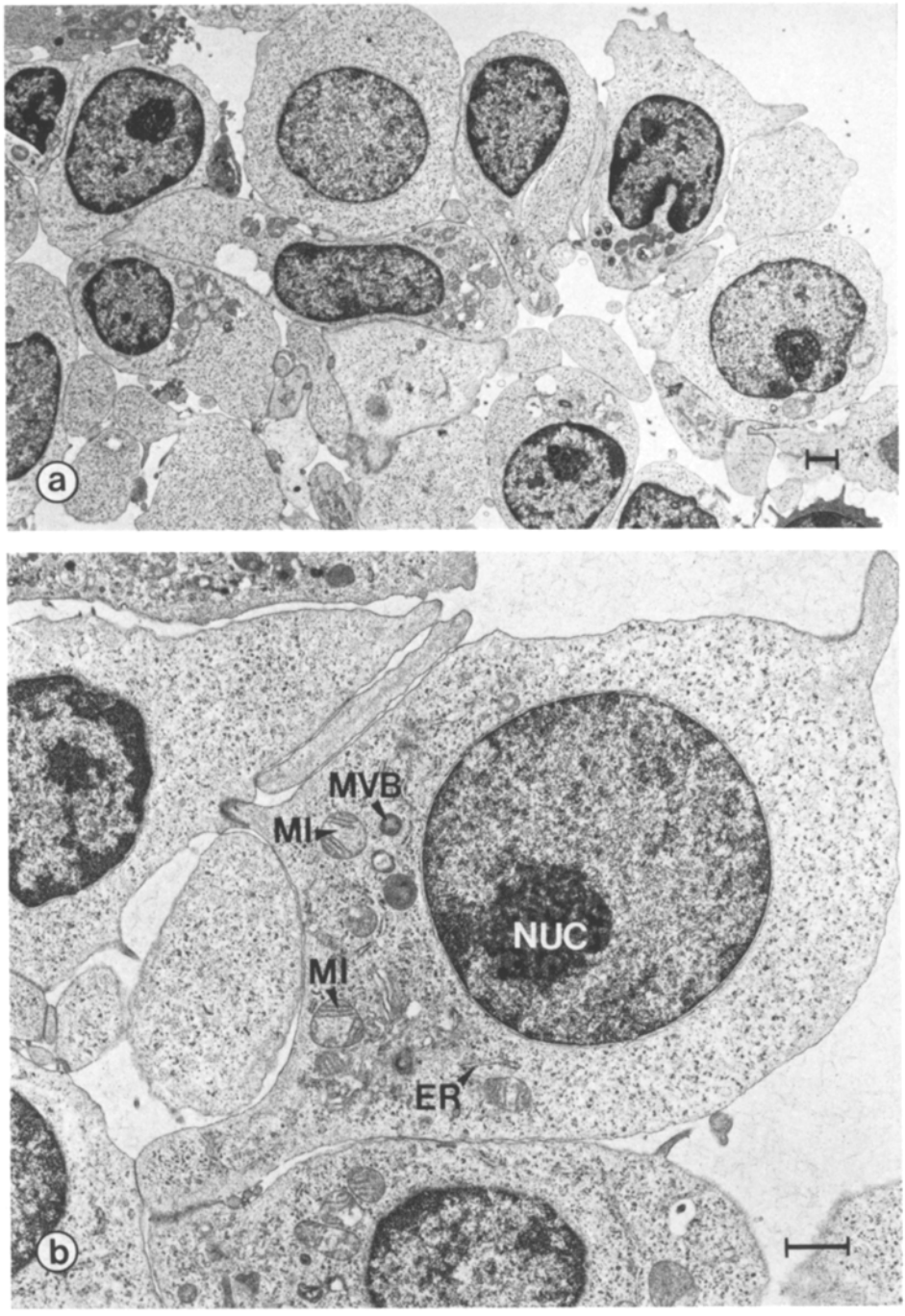

Fig. 5a and b. Ultrastructure of T-lymphocytes 24 h after PHA-stimulation. **a** The large cytoplasmic soma of most cells shows broad digitations and a few microvilli. Nuclei are rich in euchromatin. Bar, 1 μm. × 3,618. **b** The electron lucent cytoplasm contains several mitochondria (*MI*) multivesicular bodies (*MVB*) and short profiles of RER cisternae (*ER*) in a polarized arrangement. Numerous polyribosomes are diffusely throughout the cytoplasm. Bar, 1 μm. × 8,046

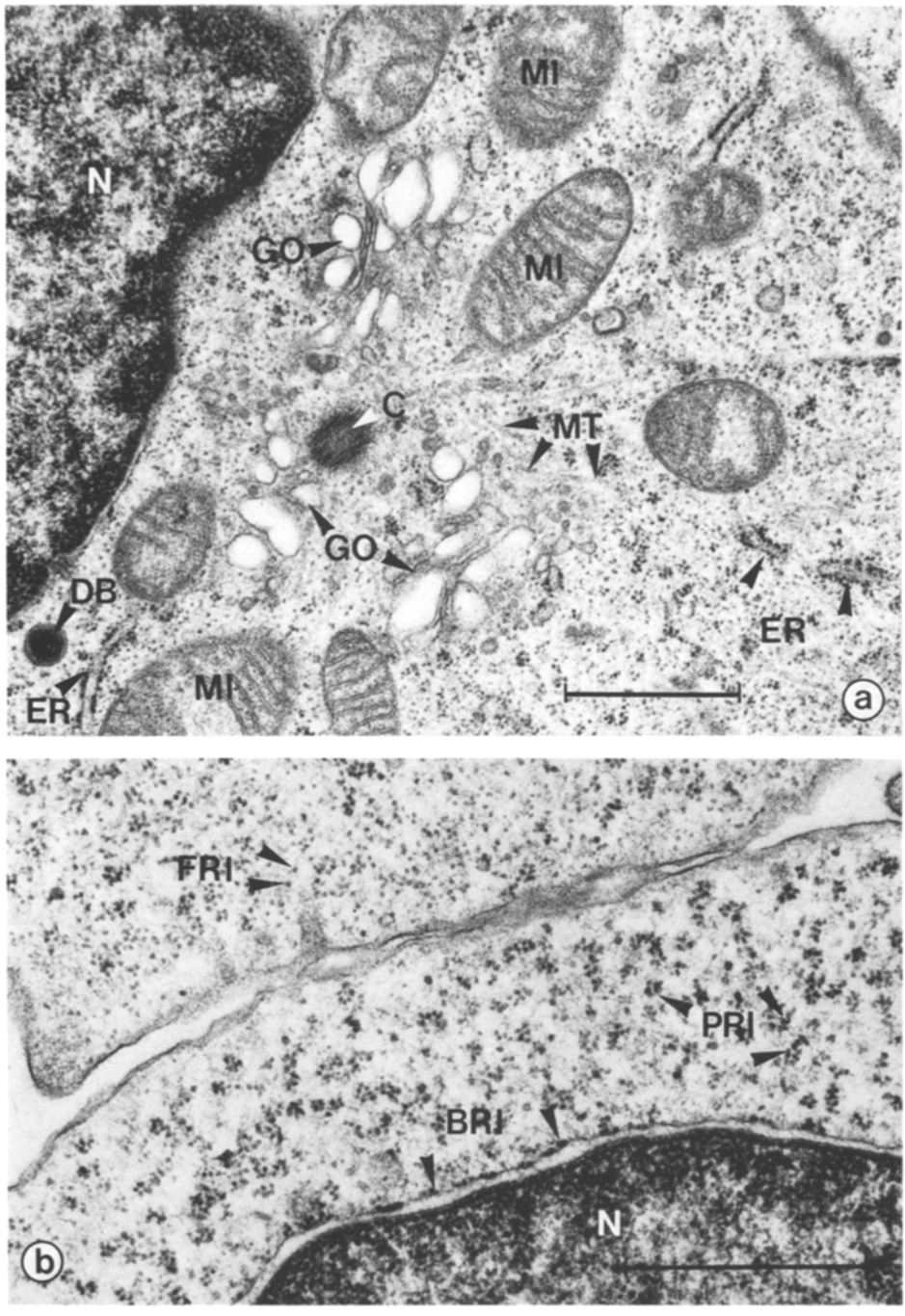

Fig. 6a and b. Ultrastructural details of T-lymphocytes 24 h after PHA-stimulation. **a** Cytoplasmic organelles such as mitochondria (*MI*), Golgi cisternae (*GO*), a centriole (*C*), a dense body (*DB*), rough endoplasmic reticulum (*ER*) and microtubuli (*MT*) are concentrated in the centrosphere. Bar, 1 μm. ×23,652. **b** The ground substance is of low electron density and contains a large number of polyribosomes (*PRI*) and fewer single free ribosomes (*FRI*). Bound ribosomes (*BRI*) are irregularly scattered along the outer aspect of the nuclear membrane. *N* nucleus. Bar, 1 μm. ×32,805

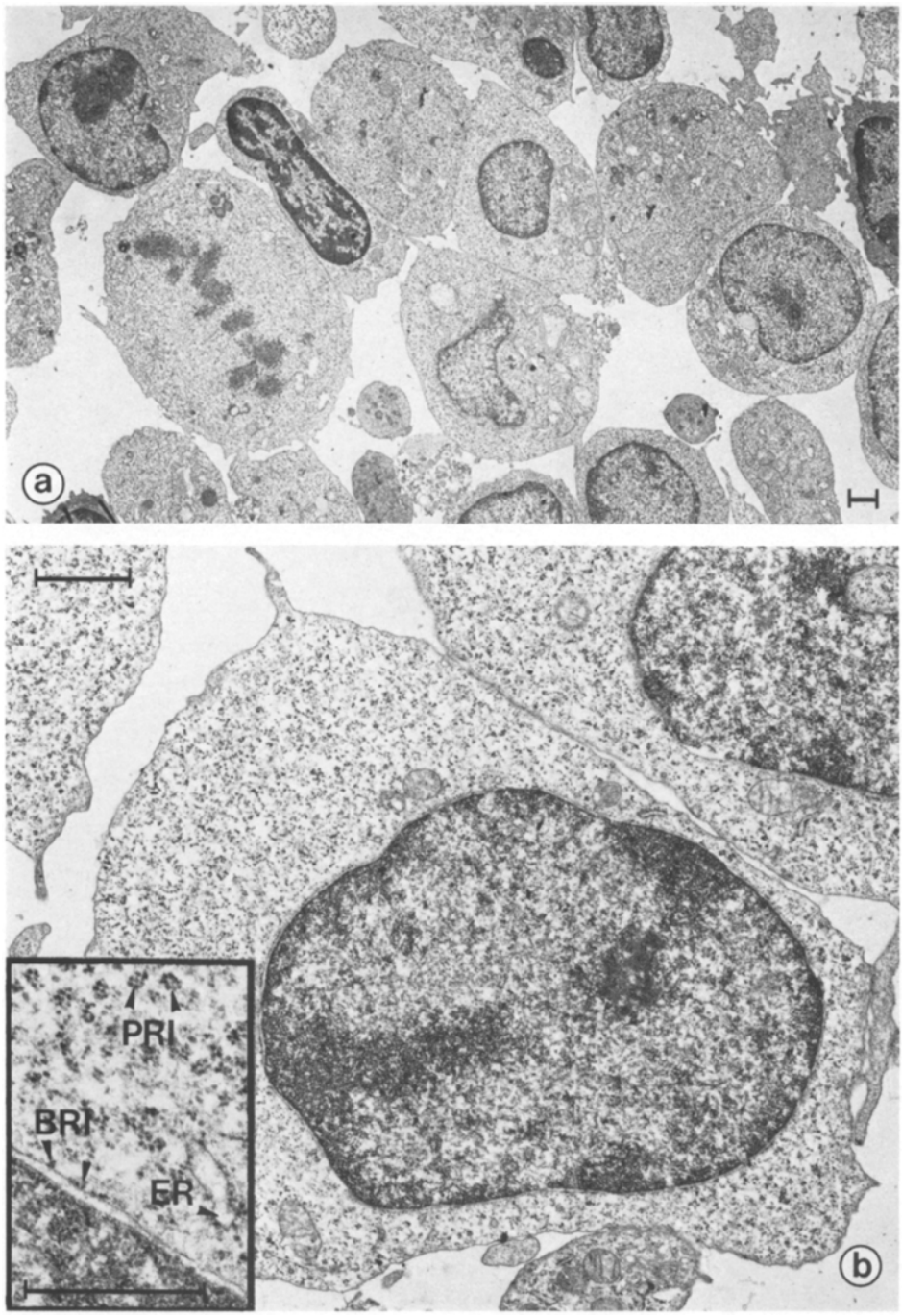

Fig. 7 a and b. Ultrastructure of a T-lymphocyte aggregate 48 h after PHA-stimulation. **a** Most cells are typical T-blasts. Note a cell in mitosis. The cytoplasm of most cells contains large, dilated mitochondria. Bar, 1 μm. × 3,618. **b** T-blast at higher magnification. Peripheral patches of heterochromatin surround the central mass of euchromatin. The cytoplasm is dominated by polyribosomes (*PRI*; inset). Bound ribosomes (*BRI*) appear in irregular fashion along the outer aspect of the nuclear membrane and at rough endoplasmic reticulum-profiles (*ER*). Bar, 1 μm. × 12,096. *Inset:* × 23,652

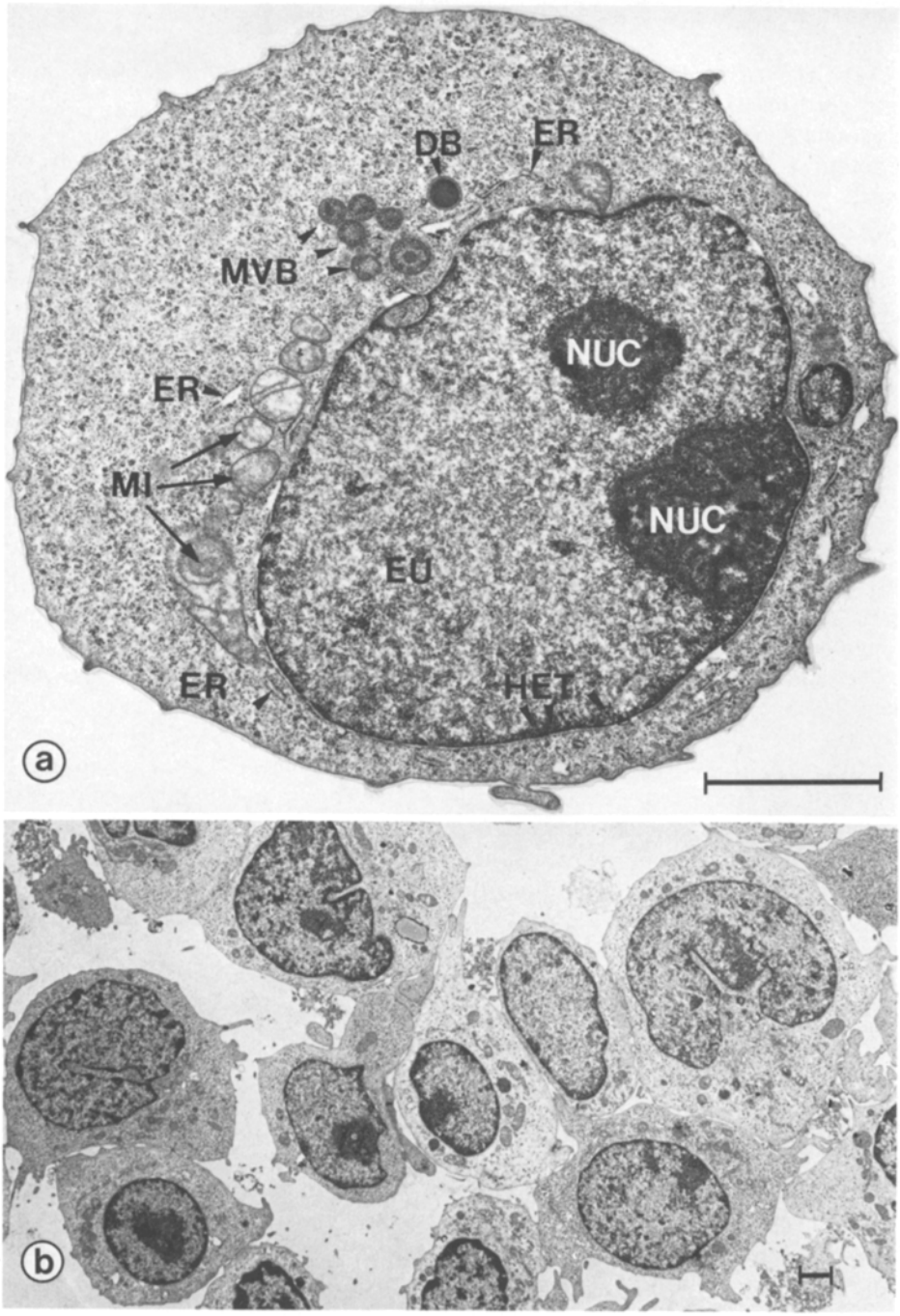

Fig. 8a and b. Ultrastructure of T-blasts 72 h after PHA-stimulation. **a** The nucleus contains little heterochromatin (*HET*), and is rich in euchromatin (*EU*); note two net-like nucleoli (*NUC*). The polarized cytoplasm includes enlarged mitochondria (*MI*) cisternae of the rough endoplasmic reticulum in a perinuclear arrangement (*ER*), a group of multivesicular bodies (*MVB*) and a dense body (*DB*). Polyribosomes are abundant. Bar, 1 μm. ×12,096. **b** A cluster of T-lymphocytes 72 h after PHA-stimulation. The cells are morphologically heterogeneous. Bar, 1 μm. ×3,618

The number of mitotic figures found in both semithin sections and cytocentrifuge smears were similar. After 24 h of activation, less than 0.1 % of the cells were dividing. Twenty-four hours later, 0.9 ± 0.3 % dividing cells occurred in semithin sections, and 0.8 ± 0.5 % in cytocentrifuge smears. After 72 h of incubation the respective data were 0.9 ± 0.4 and 0.8 ± 0.2 %. There was a marked inter-individual variability (Fig. 3).

Ultrastructure. The proportion of nuclear constituents changed greatly during activation, large aggregates of heterochromatin being replaced by granular euchromatin. Traces of heterochromatin remained marginated along the inner aspect of the nuclear envelope (Figs. 5b, 7b, 8a). Size and number of nucleoli appeared to increase, in particular after 48 h. Nucleoli of non-activated cells appeared as compact structures, while in activated cells nucleoli tended to become more reticular.

In general, the cytoplasm of T_{12}- to T_{48}-lymphocytes was less electron dense than that of T_0-lymphocytes (Fig. 4b). In T_{72}-cultures, numerous cells were still electron lucent, while others more dense (Figs. 8a, b). The number and diversity of organelles increased during activation, and most of the organelles became polarized in the centrosphere region (Figs. 5, 6a, 8a), including Golgi fields, cisternae of the rough endoplasmic reticulum (RER), lysosomal and multivesicular bodies, dense bodies and vesicles. Mitochondria changed in appearance: initially round to oval with regular cristae, they became dilated with a reduced number of cristae (Figs. 5b, 7b, 8a).

Cisternae of the RER, variably covered with ribosomes, were observed in all phases of activation and occasionally had a dilated appearance (Figs. 7b, inset; 8a). At the outer sheath of the nuclear envelope, ribosomes were usually less dense than on other RER-membranes. Dilatations were also seen in Golgi cisternae, particularly after 24 h of incubation. In contrast to dense bodies, usually single, multivesicular bodies were frequently seen in small groups (Figs. 6a, 8a). Striking alterations were noted in the development of ribosomes. At 12 h, single free ribosomes were still more numerous than polyribosomes (Fig. 4b), but the latter became increasingly more abundant at 24 h, and thereafter were regularly and densely distributed throughout the cytoplasm (Figs. 7b, 8a).

Quantitative Constitution of Activated T-Lymphocytes

The description of a changing quantitative constitution of T-lymphocytes is based on mean values. Although the cell populations used were asynchronous and varied amoung subjects, a characterization of average cells typical for certain activation periods was possible.

Cells and Nuclei. During the first 48 h of incubation, the absolute cell volume increased from 104 ± 20 to $518 \pm 31\ \mu m^3$, thereafter decreasing to $392 \pm 48\ \mu m^3$ (T_{72}; Table 1, Fig. 9). The cell surface tripled up to 48 h, while declining thereafter (Table 1). From T_0 to T_{24}, the absolute nuclear volume doubled (Fig. 10), while the cytoplasmic volume quadrupled (Fig. 11). Consequently, while nuclear volume

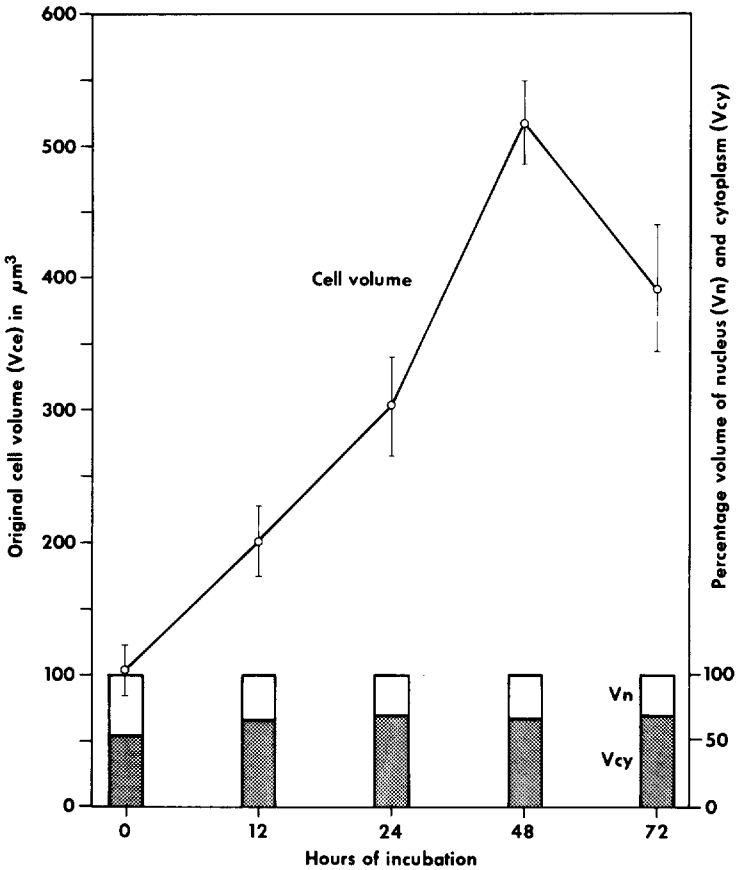

Fig. 9. Absolute average cell volume ($\bar{x} \pm s$) and its percentage nuclear and cytoplasmic fractions as a function of incubation time

density decreased (Fig. 10) and cytoplasmic volume density increased (Fig. 11), the ratio of nuclear to cytoplasmic volume fell from 0.9 ± 0.2 to 0.4 ± 0.1 (Table 1, Fig. 9). Afterwards, from T_{24} to T_{72}, the absolute nuclear and cytoplasmic volume fractions changed proportionally, i.e., the nuclear and cytoplasmic volume densities as well as the ratio of nuclear to cytoplasmic volume remained constant (Figs. 9–11). The nuclear surface doubled within the first 48 h of incubation, and later fell by about 10%. The ratio of nuclear to cell surfaces decreased up to 24 h and remained almost stable thereafter (Table 1).

During the activation period, nuclear composition changed markedly, with nucleolar and euchromatin volume fractions increasing at the expense of the heterochromatin (Table 1). The latter occupied 66.4% at T_0, and 41, 28.8 and 12.8% of the nuclear volume at T_{12} to T_{48}, respectively. Between T_{48} and T_{72}, the average nuclear composition remained rather stable (Table 1). Consequently, the ratio of eu- to heterochromatin increased from T_0 to T_{48} (Table 1).

Table 1. Stereological parameters characterizing non-activated T-lymphocytes. Average absolute data over four individuals

Components	Parameters	Non-activated small blood-derived cells			PHA-activated, cultured, 12 h		
		$\bar{x}$	$\pm s$	(R)	$\bar{x}$	$\pm s$	(R)
T-Lymphocyte							
Volume	Vce	103.8	± 19.5		201.5	± 27	
Surface	Sce	127.6	± 21.1		206.2	± 19.3	
Nucleus				0.56 ± 0.05			0.42 ± 0.02
Volume	Vn	47.9	± 9.6	(Sn/Sce)	68.4	± 5.2	
Surface	Sn	71.6	± 7.2		85.9	± 4.0	
Euchromatin							
Volume	Veu	15.6	± 3.3		38.0	± 4.7	
Heterochromatin				0.49 ± 0.02			1.36 ± 0.15
Volume	Vhet	31.8	± 6.3	(Veu/Vhet)	27.9	± 0.5	
Nucleolus							
Volume	Vnuc	0.5	± 0.2		2.5	± 0.2	
Cytoplasm				0.86 ± 0.15			0.52 ± 0.06
Volume	Vcy	55.9	± 11.8	(Vn/Vcy)	133.1	± 22.2	
Mitochondria							
Volume	Vmi	4.6	± 1.3		10.2	± 3.1	
Number	Nmi	29.6	± 10.6		47.6	± 14.0	
Size	Vmi/Nmi	16.4	± 1.9		21.9	± 0.7	
Rough endoplasmic reticulum							
Volume	Ver	0.7	± 0.2		2.1	± 0.4	
Surface	Ser	63.6	± 22.2		124.2	± 23.3	
Bound ribosomes							
Number	Nbri	260.3	± 29.8		192.5	± 44.5	
Golgi apparatus							
Volume	Vgo	0.2	± 0.1		0.5	± 0.2	
Surface	Sgo	12.6	± 5.0		26.1	± 7.3	
Vesicles							
Volume	Vves	0.06	± 0.03		0.03	± 0.03	
Number	Nves	63.0	± 45.4		70.7	± 57.6	
Size	Vves/Nves	0.1	± 0		0.1	± 0	
Lysosomes							
Volume	Vly	0.3	± 0.1		0.2	± 0.2	
Number	Nly	4.3	± 1.6		5.7	± 4.1	
Size	Vly/Nly	10.2	± 8.6		3.7	± 4.1	
Multivesicular bodies							
Volume	Vmvb	0.1	± 0.1		0.5	± 0.1	
Number	Nmvb	2.8	± 1.8		7.7	± 1.2	
Size	Vmvb/Nmvb	5.5	± 4.6		6.8	± 1.2	
Dense bodies							
Volume	Vdb	0.01	± 0.02		0.08	± 0.05	
Number	Ndb	0.6	± 0.8		2.5	± 2.2	
Size	Vdb/Ndb	0.7	± 1.3		3.0	± 2.9	
Lipid droplets							
Volume	Vld	0.05	± 0.05		0.2	± 0.2	
Number	Nld	0.3	± 0.3		1.5	± 0.6	
Size	Vld/Nld	5.5	± 5.4		14.6	± 14.2	
Glycogen							
Volume	Vgly	–			–		
Filaments							
Volume	Vfi	0.03	± 0.03		0.1	± 0.1	
Cytoplasmic ground substance							
Volume	Vcgs	49.8	± 10.3		119.2	± 22.4	
Ribosomes							
Total number	Ntri	231	± 32		446	± 148	
Free ribosomes							
Number	Nfri	202	± 30		231	± 91	
Aggregated ribosomes							
Number	Nari	29	± 6		215	± 58	
Polyribosomes							
Number	Npri	12	± 0.7		69	± 20	
Ribosomes per polyribosome	$\bar{x}$Nri/PRI	2.38			3.13		

blastforming cells									Units
24 h			48 h			72 h			
$\bar{x}$	± s	(R)	$\bar{x}$	± s	(R)	$\bar{x}$	± s	(R)	
303.0	± 37.2		518.0	± 31.4		392.3	± 47.6		μm^3
273.6	± 29.1		381.2	± 31.7		313.0	± 19.4		μm^2
		0.37 ± 0.02			0.41 ± 0.03			0.45 ± 0.07	
92.6	± 5.2		169.9	± 8.0		126.0	± 20.2		μm^3
100.5	± 5.6		153.9	± 2.5		138.8	± 17.5		μm^2
61.2	± 6.8		134.5	± 10.1		97.3	± 16.1		μm^3
		2.34 ± 0.37			6.21 ± 1.50			4.90 ± 0.18	
26.5	± 1.5		21.7	± 3.3		19.8	± 3.8		μm^3
4.9	± 0.3		13.7	± 1.0		8.9	± 1.2		μm^3
		0.45 ± 0.05			0.49 ± 0.03			0.47 ± 0.07	
210.4	± 32.1		348.1	± 25.4		266.3	± 31.9		μm^3
17.0	± 3.2		32.4	± 4.4		25.9	± 2.9		μm^3
53.5	± 11.5		67.7	± 15.3		85.0	± 14.6		Number
32.7	± 3.7		49.3	± 8.9		32.8	± 6.9		$\mu m^3 \times 10^{-2}$
3.1	± 0.7		5.4	± 0.5		4.1	± 1.4		μm^3
188.7	± 25.3		350.0	± 36.0		265.3	± 54.0		μm^2
200.2	± 26.2		216.2	± 14.9		271.0	± 23.1		Number
1.0	± 0.4		2.0	± 0.8		1.1	± 0.5		μm^3
56.7	± 19.4		94.5	± 34.8		62.3	± 2.1		μm^2
0.07	± 0.07		0.2	± 0.1		0.3	± 0.1		μm^3
135.1	± 117.6		737.5	± 565.1		331.7	± 106.7		Number
0.1	± 0		0.1	± 0		0.1	± 0		$\mu m^3 \times 10^{-2}$
0.1	± 0.1		1.6	± 0.5		0.9	± 0.6		μm^3
6.2	± 4.2		24.3	± 15.0		11.9	± 7.6		Number
1.1	± 1.2		9.8	± 5.9		8.0	± 3.3		$\mu m^3 \times 10^{-2}$
0.7	± 0.4		2.0	± 1.3		1.0	± 0.5		μm^3
10.3	± 7.9		31.4	± 17.5		14.3	± 4.7		Number
7.2	± 2.9		7.1	± 2.7		6.9	± 3.8		$\mu m^3 \times 10^{-2}$
0.1	± 0.1		0.05	± 0.04		0.3	± 0.2		μm^3
2.8	± 2.6		2.4	± 3.0		10.1	± 8.7		Number
3.0	± 4.3		0.3	± 0.4		1.8	± 1.2		$\mu m^3 \times 10^{-2}$
0.8	± 0.6		0.9	± 0.3		1.1	± 0.4		μm^3
2.4	± 0.8		4.5	± 1.6		4.3	± 1.7		Number
25.6	± 16.6		17.8	± 4.3		26.2	± 7.5		$\mu m^3 \times 10^{-2}$
–			0.04	± 0.05		0.3	± 0.3		μm^3
0.1	± 0.1		–			0.03	± 0.07		μm^3
187.4	± 28.9		303.6	± 24.5		231.3	± 28.7		μm^3
675	± 154		1,181	± 135		1,075	± 100		Number $\times 10^3$
307	± 69		568	± 96		589	± 68		Number $\times 10^3$
368	± 107		613	± 65		486	± 55		Number $\times 10^3$
108	± 27		184	± 15		155	± 23		Number $\times 10^3$
3.42			3.33			3.13			Number

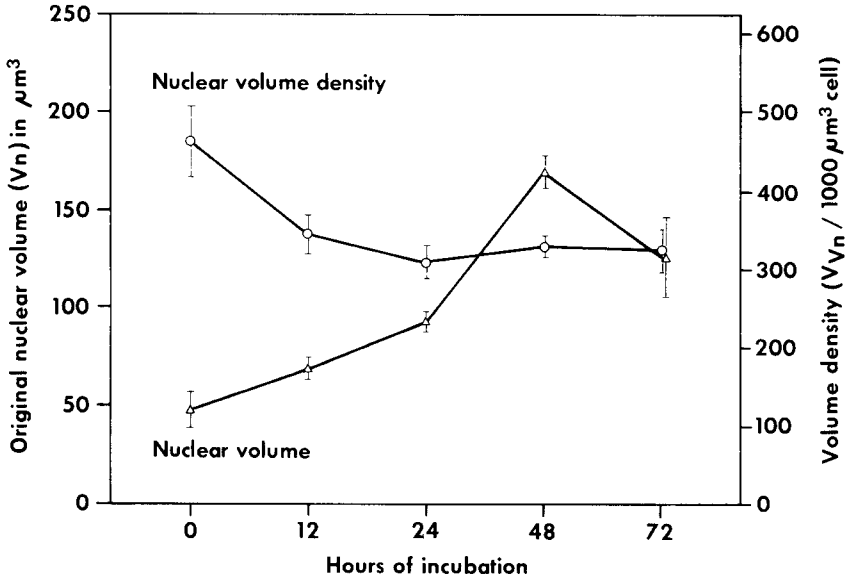

Fig. 10. Absolute average nuclear volume ($\bar{x} \pm s$) and average nuclear volume density as a function of incubation time

Cytoplasmic Constituents. The absolute volume of cytoplasm and mitochondria per cell increased in an almost proportional fashion up to 48 h and fell thereafter, while the number of mitochondria per cell rose constantly from 30 ± 11 (T_0) to a maximum of 85 ± 15 (T_{72}; Table 1). Therefore, the volume density of mitochondria expressed per unit volume of cytoplasm remained rather constant throughout the activation period, except for an insignificant increase between T_{24} and T_{48} (Fig. 12). The numerical density of mitochondria, expressed per unit volume of the cell or its cytoplasm, decreased constantly up to T_{48} and significantly increased thereafter (Fig. 12). On the average, mitochondria increased in size from $16.4 \pm 1.0\,\mu m^3$ to $49.3 \pm 8.9\,\mu m^3$, but became smaller in T_{72}-cells (Table 1).

The absolute volume and surface of the RER developed in rough proportion to the cytoplasmic volume, except for the RER-volume during the first 12 h of incubation (Table 1; Fig. 13). Consequently, the volume density of RER expressed per unit volume of cytoplasm increased from T_0 to T_{12} by about 25 % and remained stable thereafter. The respective surface density of RER was constant throughout the entire activation period, while the numerical density of bound RER-ribosomes, which decreased during the first 12 h, stabilized up to 48 h and increased significantly between T_{48} and T_{72} (Fig. 13).

Golgi Apparatus. Both the absolute volume and the surface of the Golgi apparatus reached their maximum after 48 h (Table 1). While the Golgi surface developed in proportion to the cytoplasmic volume, the Golgi volume did not, increasing in particular after 24 and 48 h, probably due to dilatation.

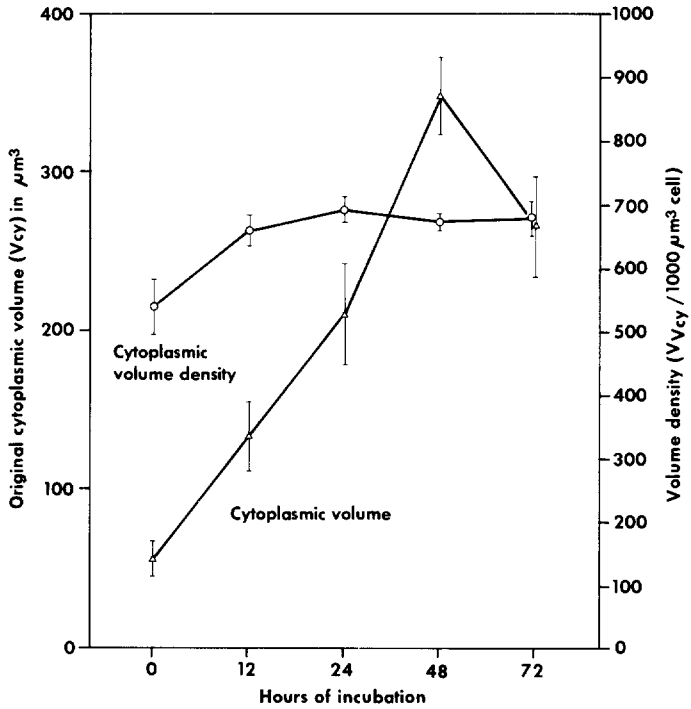

Fig. 11. Absolute average cytoplasmic volume ($\bar{x} \pm s$) and average cytoplasmic volume density as a function of incubation time

Vesicles. The absolute volume and number of vesicles varied considerably from one subject to the next (Table 1). On an average, vesicle size remained constant. Up to 24 h of incubation, the vesicle fraction did not increase, in contrast to the increase in cytoplasm. Therefore, the volume and numerical densities of vesicles fell. After 48 h of incubation, the vesicle volume had tripled and their density and number increased twelve-fold (Table 1).

Lysosomal Bodies. The changes in parameters of lysosomal bodies paralleled those of the vesicles during the entire activation period. Their number remained constant up to 24 h and increased five- to six-fold thereafter. Their size appeared to decrease during the first 24 h, but subsequently regained initial dimensions (Table 1).

Multivesicular Bodies. Both the absolute volume and number of multivesicular bodies increased up to 48 h, roughly in proportion to the cytoplasmic volume (Table 1). Volume and numerical density per unit volume of the cell and the cytoplasm remained rather stable, except for a slight increase in T_{48}-cells. The size of multivesicular bodies increased slightly during the first 24 h of incubation, remaining constant thereafter.

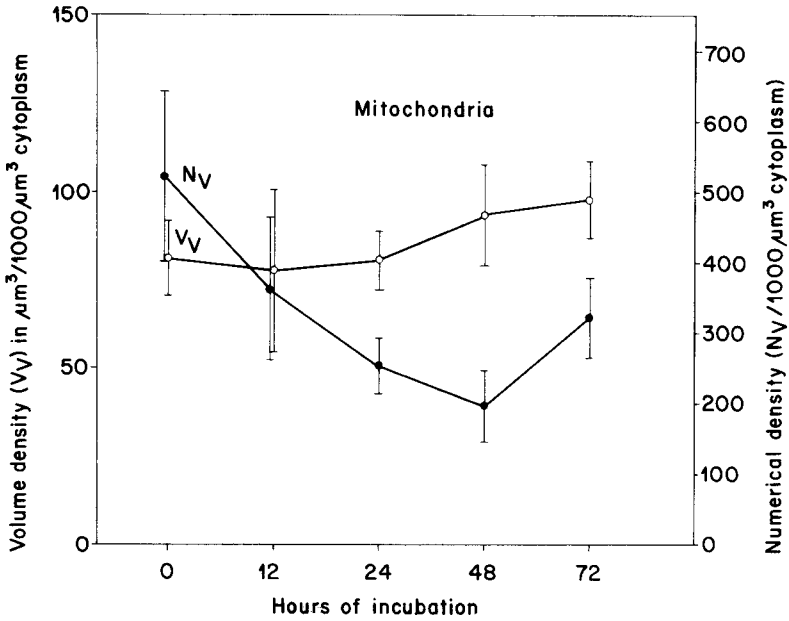

Fig. 12. Average volumetric and numerical density ($\bar{x} \pm s$) of mitochondria as a function of incubation time

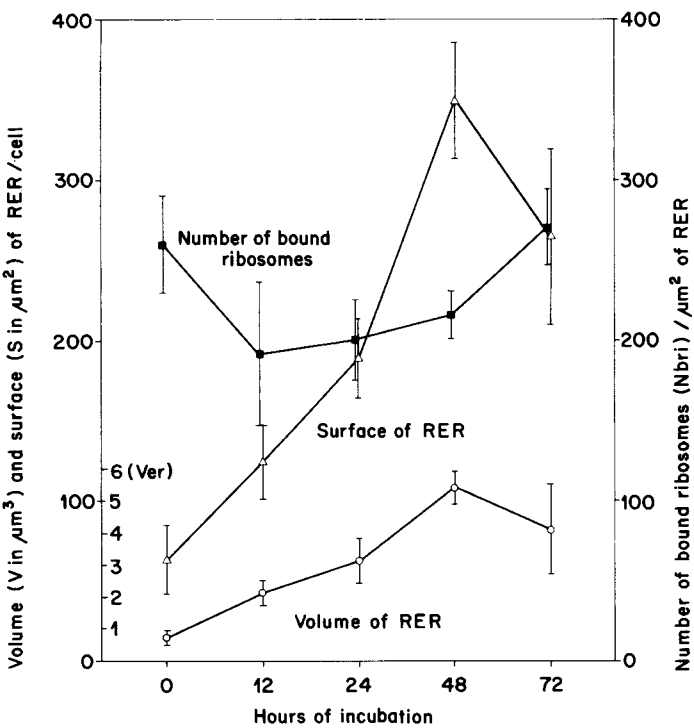

Fig. 13. Average density of bound ribosomes/μm^2 RER and absolute volume and surface ($\bar{x} \pm s$) of the rough endoplasmic reticulum as a function of incubation time

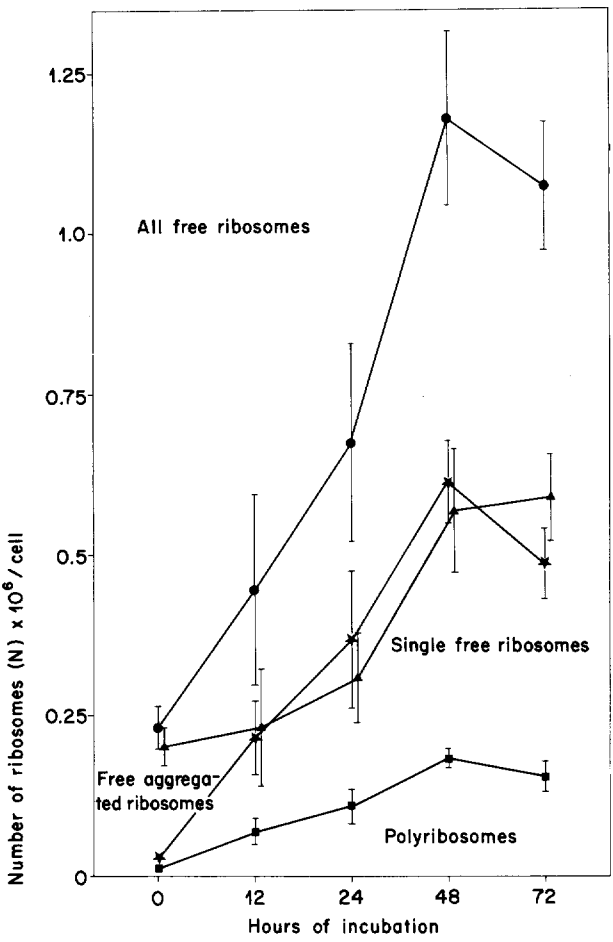

Fig. 14. Average absolute number ($\bar{x} \pm s$) of all free ribosomes (*dots*), and of single, free ribosomes (*triangles*), free, aggregated ribosomes (*stars*) and polyribosomes (*squares*) per cell as a function of incubation time

Dense Bodies. Absolute volume, as well as volume and numerical density parameters varied greatly among subjects. None of these parameters appeared to change significantly (Table 1).

Lipid Droplets. The absolute volume and size increased continuously during the first 24 h of incubation. The absolute number of lipid droplets increased significantly during the first 12 h and between 24 h and 48 h (Table 1). Consequently, volume and numerical density parameters per unit volume of the cell and the cytoplasm approximately doubled during the first 12 h, while later the numerical density remained stable and the volume density further increased between 12 and 24 h.

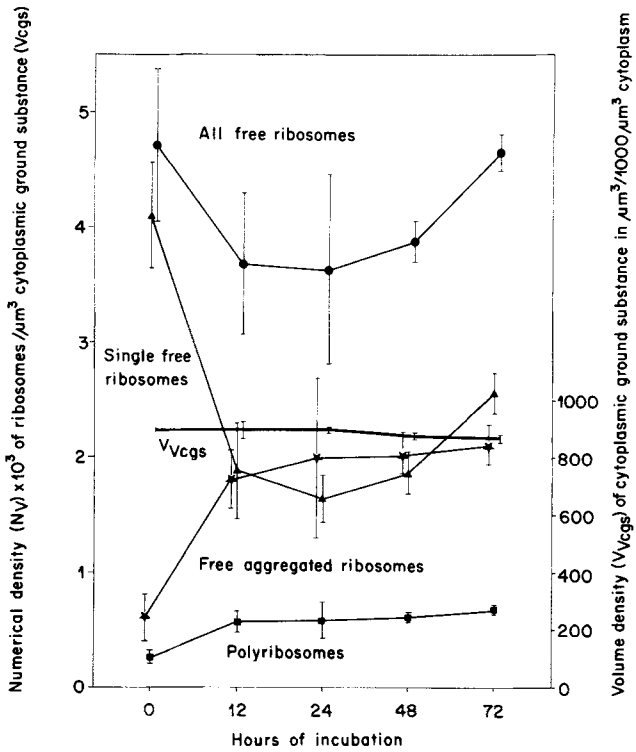

Fig. 15. Average numerical density ($\bar{x} \pm s$) of all free ribosomes (*dots*), and of single, free ribosomes (*triangles*), free, aggregated ribosomes (*stars*) and polyribosomes (*squares*) related to 1 μm^3 cytoplasmic ground substance, as well as average volume density ($\bar{x} \pm s$) of the cytoplasmic ground substance (related to a unit volume of cytoplasm) as a function of incubation time

Glycogen Granules and Cytoplasmic Filaments. Glycogen granules were observed only after 48 h and occupied very small volume fractions. Cytoplasmic filaments were present, although rare, at all time points of activation (Table 1).

Free Ribosomes. The absolute number of all free ribosomes increased in parallel to the cytoplasmic volume, both reaching maxima of about six-fold of the initial values at 48 h of incubation. The number of single, free ribosomes did not change during the first 12 h, increased slightly to T_{24} and rapidly to T_{48}, with no change from T_{48} to T_{72} (Table 1, Fig. 14). The number of aggregated ribosomes increased rapidly and continuously up to 48 h of incubation, while the number of polyribosomes rose continuously but more slowly (Fig. 14). The absolute number of aggregated ribosomes constituting a polyribosome increased mainly during the first 12 h of incubation (Table 1). The volume density of the cytoplasmic ground substance expressed per unit volume of cytoplasm was stable throughout the activation period (Fig. 15). When calculated in relation to a unit volume of ground substance or cytoplasm, the numerical density of single free ribosomes decreased markedly during the first 12 h of incubation and subsequently remained at the reduced level up to 48 h, with a final increase in T_{72}-cells. On the other hand, the

Table 2. ^{3}H-thymidine-uptake of human PHA-activated lymphocytes and of nonactivated control lymphocytes, 12, 24, 48 and 72 h after stimulation

No. Donors	^{3}H-dThd-uptake (dpm ± s)							
	12 h		24 h		48 h		72 h	
	PHA-P	control	PHA-P	control	PHA-P	control	PHA-P	control
1	47 ± 25	40 ± 21	142 ± 102	48 ± 22	55,315 ± 3,921	154 ± 56	137,468 ± 9,384	84 ± 54
2	58 ± 40	43 ± 26	245 ± 52	82 ± 30	14,039 ± 3,109	142 ± 128	48,643 ± 8,802	191 ± 61
3	99 ± 64	123 ± 53	467 ± 146	88 ± 38	18,620 ± 1,022	123 ± 78	57,763 ± 5,690	43 ± 33,5
4	189 ± 186	182 ± 102	219 ± 125	95 ± 67	21,385 ± 1,697	72 ± 18	54,819 ± 4,197	–

Data represent averages ± SD derived from 12 parallel cultures each

Table 3. ^{3}H-leucine-uptake of human PHA-activated lymphocytes and of nonactivated control lymphocytes, 12, 24, 48 and 72 h after stimulation.

No. donors	^{3}H-leucine-uptake (dpm ± s)							
	12 h		24 h		48 h		72 h	
	PHA-P	control	PHA-P	control	PHA-P	control	PHA-P	control
1	1,521 ± 291	683 ± 230	2,749 ± 323	560 ± 103	24,908 ± 1,076	1,025 ± 357	45,307 ± 4,689	672 ± 148
2	1,956 ± 395	718 ± 168	3,463 ± 309	845 ± 193	6,621 ± 2,373	751 ± 514	21,475 ± 2,063	569 ± 365
3	1,819 ± 391	691 ± 113	2,893 ± 451	568 ± 138	9,380 ± 604	664 ± 156	22,725 ± 1,660	470 ± 148
4	1,371 ± 258	795 ± 258	2,037 ± 352	965 ± 430	7,180 ± 583	672 ± 178	22,453 ± 2,648	–

Data represent averages ± SD derived from 12 parallel cultures each

numerical density of free aggregated ribosomes and of polyribosomes increased significantly during the first 12 h, with no change thereafter (Fig. 15).

^{3}H-Thymidine and ^{3}H-Leucine Uptake

The ^{3}H-thymidine uptake started 24 h after stimulation and reached a maximum at 72 h in all four subjects. However, T_{48}- and T_{72}-cells of subjects 2, 3 and 4 revealed a two- to three-fold less isotope uptake than subject 1 (Table 2).

Uptake of ^{3}H-leucine started 12 h after stimulation and, in all four subjects, rose slightly up to 24 h of incubation. T_{48}- and T_{72}-cells of subjects 2, 3 and 4 took up about two- to three-fold less isotope than did subject 1 (Table 3). In both tests, control values remained rather stable (Tables 2, 3).

Cytotoxicity Assay

The kinetics of the cytotoxic effect of supernatants originating from PHA-stimulated and non-stimulated T-lymphocytes on α-L-fibroblasts are illustrated in

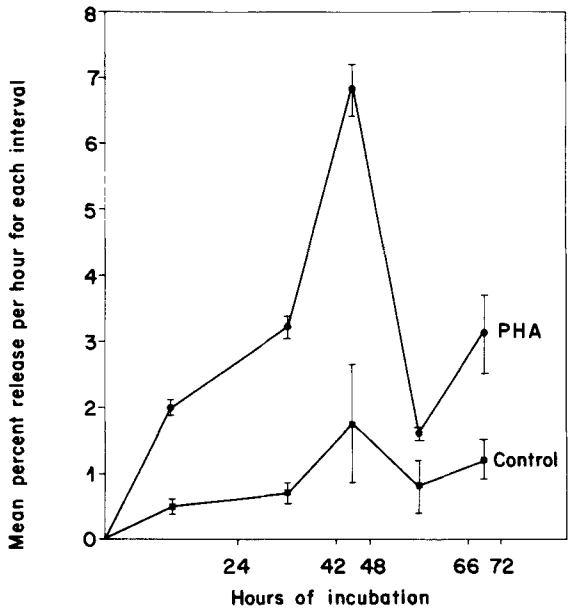

Fig. 16. Kinetics of the cytotoxic effect of PHA-stimulated and non-stimulated T-lymphocyte-supernatants on α-L-fibroblasts as a function of the time periods of T-lymphocyte incubation. Percentage ^{51}Cr-release was calculated per incubation hour and plotted at time interval midpoints. Corresponding measurements performed on supernatants of non-activated T-lymphocytes served as controls

Figure 16. The ^{51}Cr-release (PR) increased during the first 45 h of incubation (2.05 ± 0.13 at 12 h, 3.23 ± 0.22 at 33 h, 6.12 ± 0.44 at 45 h). Later on, the PR declined (1.58 ± 0.08 at 57 h) and rose again (3.14 ± 0.63 at 96 h). All of these data were different from the respective control values (Fig. 16).

Discussion

The present investigation, relating morphological and stereological observations to biochemical data, characterizes the activation process of PHA-stimulated T-lymphocytes. Because of the high degree of purity of the T-lymphocyte populations used, activated cells revealed rather homogeneous morphology, and their characteristic features resembled those of mammalian T-blasts described by other authors (Biberfeld, 1971 b; Douglas, 1971; Janossy et al. 1972). However, our T-cell preparations included a number of immunologically different subgroups (Evans et al., 1977; Grossie et al., 1978; Matter et al., 1972) which could not be distinguished morphologically. Typical B-blasts were excluded from counting. Subject variability was observed in all data obtained, including variations in lymphocyte proliferation as observed previously (Osa and Weksler, 1977). In particular, considerable variations of stereological data were probably due to difficulties in precise recognition and identification of some organelles, such as lysosomal bodies,

multivesicular and dense bodies, or vesicles, particularly because no labeling was performed. Evaluation of organelles smaller than a section thickness of 54 nm (i.e., ribosomes, glycogen storage granules and cytoplasmic filaments) was only approximate. An underestimation of polyribosomes may have occurred as a consequence of tangential sectioning which results in imperfect grouping.

The stereological test system and data processing (CELLANAL; Petrzilka et al., 1978) employed the original average cell volume of T-lymphocytes as the basic reference compartment. Therefore, precise estimation of this reference volume was most critical (Petrzilka et al., 1978). A comparison of average cell volume data obtained either by Coulter Counter measurements or by stereological techniques revealed parameter identity except for small, insignificant variations. Because of methodological differences and differences in the cell populations used, the size and other data of the present T-cell populations, reached after various periods of incubation, cannot be compared to data reported by other authors (Biberfeld, 1971 b; Douglas et al., 1973; Konwinski and Kozlowski, 1972).

A number of our data on T-lymphocyte activation corroborated and strengthened that of previous investigations. The changes of nuclear constituents with time proceeded as reported by Biberfeld (1971 b). Replacement of large volume fractions of heterochromatin by euchromatin in T_{12}-cells indicated that structural changes preceded the ^{3}H-thymidine uptake. The ratio of eu- to heterochromatin after 64 h of incubation, reported in a previous study (Hirschhorn et al., 1971), was higher than our maximal value at T_{48}, which had dropped at T_{72} but was not determined between T_{48} and T_{72}. The structural and volumetric changes of the nucleolus, observed during the first 24 h of incubation, corresponded also to data previously reported (Biberfeld, 1971 b). In the latter study as well as in the present investigation, a nucleolar diameter increase of two to three times and a respective volume increase of roughly ten times was established.

Cytoplasmic organelles, in particular their volume fractions, did not always develop in proportion to volume changes of the entire cytoplasm. For example, within the first 48 h after stimulation, the total mitochondrial volume fraction had increased in parallel with the cytoplasmic volume, while the absolute number of mitochondria had not. In our material, a T_{24}-cell contained, on the average, 54, a T_{48}-cell 68 and a T_{72}-cell 85 mitochondria. On the basis of counts in histochemically treated smear preparations, Biberfeld (1971 b) found 50 to 100 mitochondria/cell for medium and large lymphocytes. The average size of single mitochondria, however, rose disproportionally to their number and declined after 48 h. These data imply that (i) the decreasing numerical density of mitochondria up to 48 h was the consequence of a cytoplasmic development in excess of the rate of mitochondria formation; (ii) the increase in absolute volume of his organelle per cell was due to an enlargement of mitochondrial size. Newly formed mitochondria probably appeared only after T_{48}. Thus, the increase of their numerical density in the cytoplasm between T_{48} and T_{72} correlated with a decrease in organelle size, resulting in a declining absolute volume fraction of mitochondria per cell. Consequently, because of the absolute cell and cytoplasmic volume decreasing between 48 and 72 h, the eventual volume density of mitochondria per cell or cytoplasm rose. The volume of RER cisternae, from T_0 to T_{12}, increased disproportionally to, and later on in parallel with the cytoplasmic volume. The

latter was always in phase with the increase of RER membrane formation. The discrepancy between volume and surface in the initial RER development was due to dilatation of its cisternae. While the RER membrane system became enlarged, the density of bound ribosomes decreased. In morphological terms, the Golgi cisternae appeared to become dilated as well. However, based on stereological data, the increase of both Golgi membranes and volume of Golgi cisternae was proportional with that of the cytoplasmic volume.

Proteins, for example lymphotoxins, being synthesized in the RER cisternae, were probably concentrated in the Golgi apparatus and then transported by vesicles. The lymphotoxin release, in the present study, was at its maximum 48 h after incubation, when both volume and surface parameters of the RER were at their peak. However, the increase in the number of vesicles per cell and their numerical density in the cytoplasm did not correlate with the lymphotoxin release. Functional correlations between RER, Golgi apparatus, vesicles and lysosomal structures were described by Biberfeld (1971a), who proposed a connection between the biogenesis of lysosomal structures and the increasing endocytosis of activated cells. He suggested that endocytotic vesicles may convert to multivesicular bodies and the latter to dense bodies. Data of this study do not corroborate these suppositions, except for the fact that after 72 h of incubation the maximal number of dense bodies followed a maximal number of multivesicular bodies observed in T_{48}-cells.

Estimation of the percentages of activated and dividing lymphocytes indicated that the majority of PHA-stimulated cells became activated, but only a few (1 %) divided. These findings corroborate those of other authors who studied human and mouse mixed-lymphocytes (Harris and Olsen, 1976; Rogers et al., 1972). The fact that most parameters decreased from T_{48}- to T_{72}-cells may be attributed to the increase in mitotic activity observed in T_{48}-cells and the resulting multiplication of daughter cells. This view appears to be in line with the increasing uptake of the thymidine isotope 48 h after incubation. Under the applied culture conditions, this isotope uptake would probably have declined soon after 72 h (Nowell et al., 1974), since a non-dialyzable factor, obtained from extracts of routine PHA-cultures, apparently inhibits further proliferation of lymphocytes (Winger et al., 1977).

The results of the cytotoxicity assay also seemed to indicate that a mitotic burst had occurred prior to 48 h of incubation. It appears that the lymphotoxin release is independent of DNA-synthesis (Greaves et al., 1973; Younkin, 1975) and occurs primarily during the G_1-phase (Valdimarsson, 1976). The ^{51}Cr-release measurements were not performed in parallel with the determination of isotope uptake. Therefore, the present data did not allow estimation of the onset of the S-phase. However, previous observations (Jasinska et al., 1970; Sören, 1973) and our ^{3}H-thymidine uptake measurements, in combination, indicated a beginning of the S-phase not earlier than 24 h after incubation. Assuming a cell cycle lasts about 18 h (Younkin, 1975), a mitotic phase could hardly be expected prior to about 35 h after culture initiation. Any proposition that the slowly increasing cytotoxic effect (between 12 and 33 h) may be due to the increasing number of lymphocytes entering the S-, G_2- or mitotic phases is refuted by the concomitantly continuing increase in ^{3}H-thymidine uptake.

The early increase in ^{3}H-leucine uptake coincided with a steep rise in density of

aggregated ribosomes and polyribosomes. These findings confirm data of Ahern and Kay (1975) who, in non-activated lymphocytes, found that 25% of all ribosomes were actively synthesizing protein, while already 12 h after PHA-stimulation 80% of all ribosomes were carrying out this activity. Initially, during the first 12 h of activation, the lymphocytes are capable on enhanced protein synthesis without and prior to formation of new ribosomes (Kay et al., 1971). Obviously, this is accomplished through an increase in the number of polyribosomes at the expense of free, already existing ribosomes. This statement, based on the present stereological data, directly corroborates the biochemical findings after density gradient sedimentation of Cooper (1977) and Cooper and Braverman (1977), who distinguished between free ribosomes, monosomes, and polysomes, and stated that "the larger free ribosome pool of resting lymphocytes is thus an essential source of components for accelerated protein synthesis early in lymphocyte activation, before increased synthesis can provide a sufficient number of new ribosomes". In the present study, after 12 h of activation, the numerical density of all free ribosomes became stabilized, probably because of the now increasing ribosome production. When compared to the biochemical findings of Cooper (1977), our data revealed only slight differences regarding the percentages of free ribosomes and polyribosomes found in T_{48}-cells.

When dpm-data for ^{3}H-leucine/culture were recalculated as dpm/cell (dead cells not taken into account), a continuous increase up to the end of the incubation period was encountered ($T_{12} = 0.016$, $T_{24} = 0.028$, $T_{48} = 0.12$, $T_{72} = 0.29$). These data were significantly ($P < 0.01$) and positively correlated with the polyribosome density per unit volume of cytoplasmic ground substance, implying that the degree of ^{3}H-leucine uptake is directly proportional to the number of existing polyribosomes, i.e., polyribosome density determines the rate of protein synthesis.

Polyribosomes with two or three ribosomes per polysome were observed most frequently in this study. This is in agreement with histometrical data of Sören and Biberfeld (1973). Furthermore, the most obvious increase in the number of ribosomes/polysome occurred during the first 12 h of activation, when the percentages of free and aggregated ribosomes shifted from 87.5 and 12.5 to 52 and 48, respectively. In T_{72}-cells, these data amounted to 55 and 45%, respectively, confirming the results of Chapman et al. (1967). However, guinea pig lymphoblasts, following a delayed hypersensitivity reaction, showed a different ribosome distribution (De Petris et al., 1966). Only 5 to 10 percent of all ribosomes were single, while polyribosomes were mainly comprised of four to five ribosomes. On the other hand, the absolute number of ribosomes per T_{72}-cell (1.1×10^6) was in agreement with results of Sören and Biberfeld (1973).

Acknowledgements. The authors wish to thank Dr. R. Burkart, Dr. W. Pepersack, Dr. E. Rudolf and Mr. Th. Schmid for contributing blood samples. They are indebted to Dr. R.C. Page (Center for Research in Oral Biology, University of Washington, Seattle, Wash., USA) for performing the lymphotoxin-release experiments, to Dr. G.M. Granger (Department of Biochemistry, University of California, Irvine, Ca., USA) for donating the α-L-fibroblasts, and to Dr. J.J. Burckhardt for methodological advice. The authors are particularly grateful to Mrs. A. Schwarzenbach, Mrs. A. Lardelli and Mrs. K. Rossinsky for excellent technical assistance. This study was in part supported by a Grant (NO 106) from the Hartmann-Müller-Stiftung for Medical Research and by a Grant (1975) from the Stiftung für Wissenschaftliche Forschung an der Universität Zürich.

References

Ahern, Th., Kay, J.E.: Protein synthesis and ribosome activation during the early stages of phytohemagglutinin lymphocyte stimulation. Exp. Cell Res. **92,** 513–515 (1975)

Biberfeld, P.: Endocytosis and lysosome formation in blood lymphocytes transformed by phytohemagglutinin. J. Ultrastruct. Res. **37,** 41–68 (1971a)

Biberfeld, P.: Morphogenesis in blood lymphocytes stimulated with phytohemagglutinin (PHA). A light and electron microscopic study. Acta Pathol. Microbiol. Scand., Suppl. **223** (1971b)

Biberfeld, P., Johansson, A.: Contact areas of cytotoxic lymphocytes and target cells. An electron microscopic study. Exp. Cell Res. **94,** 79–87 (1975)

Burckhardt, J.J., Guggenheim, B., Hefti, A.: Are Actinomyces viscosus antigens B cell mitogens? J. Immunol. **118,** 1460–1465 (1977)

Chapman, J.A., Elves, M.W., Gough, J.: An electron-microscopic study of the in vitro transformation of human leucocytes. I. Transformation of lymphocytes to blastoid cells in the presence of phytohemagglutinin. J. Cell Sci. **2,** 359–370 (1967)

Cooper, H.L.: Ribosome utilization and regulation of protein synthesis during lymphocyte activation. In: Regulatory mechanism in lymphocyte activation (D.O. Lucas, editor), pp. 94–113. New York, San Francisco, London: Academic Press 1977

Cooper, H.L., Braverman, R.: Free ribosomes and growth stimulation in human peripheral lymphocytes: Activation of free ribosomes as an essential event in growth induction. J. Cell. Physiol. **93,** 213–226 (1977)

Douglas, St.D.: Human lymphocyte growth in vitro: Morphologic, biochemical and immunologic significance. Int. Rev. Exp. Pathol. **10,** 41–114 (1971)

Douglas, St.D., Cohnen, G., Brittinger, G.: Ultrastructural comparison between phytomitogen transformed normal and chronic lymphocytic leukemia lymphocytes. J. Ultrastruct. Res. **44,** 11–26 (1973)

Evans, R.L., Breard, J.M., Lazarus, H., Schlossman, S.F., Chess, L.: Detection, isolation, and functional characterization of two human T-cell subclasses bearing unique differentiation antigens. J. Exp. Med. **145,** 221–233 (1977)

Greaves, M.F., Owen, J.J.T., Raff, M.C.: T and B Lymphocytes: Origins, properties and roles in immune responses. Amsterdam: Exerpta Medica; New York: American Elsevier Publ. Co., Inc. 1973

Grossi, C.E., Webb, S.R., Zicca, A., Lydyard, P.M., Moretta, L., Mingari, M.C., Cooper, M.D.: Morphological and histochemical analyses of two human T-cell subpopulations bearing receptors for IgM or IgG. J. Exp. Med. **147,** 1405–1417 (1978)

Harris, G., Olsen, I.: Cell division and deoxyribonucleic acid (DNA) synthesis in cultures of stimulated lymphocytes. Immunology **31,** 195–204 (1976)

Hirschhorn, R., Decsy, M.I., Troll, W.: The effect of PHA stimulation of human peripheral blood lymphocytes upon cellular content of euchromatin and heterochromatin. Cell. Immunol. **2,** 696–701 (1971)

Janossy, G., Shohat, M., Graves, M.F., Doumashkia, R.R.: Lymphocyte activation: IV. The ultrastructural pattern of response of mouse T- and B-cells to mitogenic stimulation in vitro. Immunology **24,** 211–227 (1972)

Jasinska, J., Steffen, J.A., Michalowski, A.: Studies on in vitro lymphocyte proliferation in cultures synchronized by the inhibition of DNA synthesis. II. Kinetics of the initiation of the proliferative response. Exp. Cell Res. **61,** 331–341 (1970)

Kay, J.E., Ahern, Th., Atkins, M.: Control of protein synthesis during the activation of lymphocytes by phytohemagglutinin. Biochem. Biophys. Acta **247,** 322–334 (1971)

Konwinski, M., Kozlowski, T.: Morphometric study of normal and phytohemagglutinin-stimulated lymphocytes. Z. Zellforsch. **129,** 500–507 (1972)

Ling, N.R., Kay, J.E.: Lymphocyte stimulation. Amsterdam-Oxford: North-Holland Publ. Co. 1975

Matter, A., Lisowska-Bernstein, B., Ryser, J.E., Lamelin, J.P., Vasalli, P.: Mouse thymus-independent and thymus-derived lymphoid cells. II. Ultrastructural studies. J. Exp. Med. **136,** 1008–1030 (1972)

Moretta, L., Webb, S.R., Grossi, C.E., Lydyard, P.M., Cooper, M.D.: Functional analysis of two human T-cell populations: help and suppression of B-cell responses by T-cells bearing receptors for IgM or IgG. J. Exp. Med. **146,** 184–200 (1977)

Nowell, P.C., Daniele, R.P., Winger, L.A.: Kinetics of human lymphocyte proliferation: Proportion of cells responsive to phytohemagglutinin and correlation with E rosette formation. J. Reticuloendothel. Soc. **17,** 47–56 (1974)

Osa, S.R., Weksler, M.E.: Demonstration of significant differences in the proliferative capacity of lymphocytes from normal human subjects. Cell. Immunol. **32,** 391–399 (1977)

Peter, H.H., Feldman, J.D.: Cell-mediated cytotoxicity during rejection and enhancement of allogeneic skin grafts in rats. J. Exp. Med. **135,** 1301–1315 (1972)

Petris, S. De, Karlsbad, G., Pernis, B., Turk, J.L.: Ultrastructure of cells present in lymph nodes during the development of contact sensitivity. Int. Arch. Allergy **29,** 112–130 (1966)

Petrzilka, G.E., Graf-de Beer, M., Schroeder, H.E.: Stereological model system for free cells and baseline data for human peripheral blood-derived small T-lymphocytes. Cell Tissue Res. **192,** 121–142 (1978)

Rogers, J.C., Boldt, D., Kornfeld, S., Skinner, A., Valeri, C.R.: Excretion of deoxyribonucleic acid by lymphocytes stimulated with phytohemagglutinin or antigen. Proc. Natl. Acad. Sci. U.S.A. **69,** 1685–1689 (1972)

Sören, L.: Variability of the time at which PHA-stimulated lymphocytes initiate DNA synthesis. Exp. Cell Res. **78,** 201–208 (1973)

Sören, L., Biberfeld, P.: Quantitative studies on RNA accumulation in human PHA-stimulated lymphocytes during blast transformation. Exp. Cell Res. **79,** 359–367 (1973)

Spofford, B.T., Daynes, R.A., Granger, G.A.: Cell-mediated immunity in vitro: A highly sensitive assay for human lymphotoxin. J. Immunol. **112,** 2111–2116 (1974)

Takahashi, A.: Karyometric and cytophotometric studies on nucleic acids in the culture of human lymphocytes with phytohemagglutinin. Virchows Archiv [Cell Pathol.] **21,** 299–311 (1976)

Valdimarsson, H.: Effector mechanisms in cellular immunity. In: The immune system. M.J. Hobart and I. McConnell, editors, pp. 179–196. Oxford, London, Edinburgh, Melbourne: Blackwell Scientific Publ. 1976

Wedner, H.J., Parker, C.W.: Lymphocyte activation. Prog. Allergy **20,** 195–300 (1976)

Winger, L.A., Nowell, P.C., Daniele, R.P.: Sequential proliferation induced in human peripheral blood lymphocytes by mitogen. I. Growth of 1000 lymphocytes in feeder layer cultures. J. Immunol. **118,** 1763–1767 (1977)

Younkin, L.H.: In vitro response of lymphocytes to phytohemagglutinin (PHA) as studied with antiserum to PHA. Exp. Cell Res. **90,** 374–380 (1975)

Accepted June 17, 1979